

Research on Parameter Identification Method for Robotic Manipulators Joint Friction Model Based on PINN

Di Luo, Zhiqin Cai, Da Jiang and Haijun Peng

Abstract— In the research and application of robotic manipulator systems, the friction phenomenon poses challenges to system stability and control precision. To further improve the parameter identification accuracy in traditional friction modeling for robotic manipulators, this paper proposes a friction model parameter identification method based on the Physics Informed Neural Network (PINN). The proposed method takes the relative velocity and normal pressure in the motion of the robotic manipulators as the information input items, with the friction and model parameters as outputs. The network parameters and identification parameters are updated according to the Adam method, achieving a more precise identification of friction parameters. It comprehensively considers friction mechanism information and data information to jointly construct the objective optimization function. Through simulation comparisons with noisy/noise-free data, the PINN method is validated to have higher identification accuracy than Genetic Algorithm (GA) and Particle Swarm Optimization (PSO), with an average reduction of 30% and 50% in the identification error rates for noise-free and noisy data, respectively.

I. INTRODUCTION

With the rapid advancement of robotics technology, a large number of robotic manipulators have been deployed in the manufacturing sector [1], significantly enhancing production efficiency through tasks such as welding, handling, and painting. Moreover, the utilization of robotic manipulators in precision machining and manufacturing has been increasingly prevalent, necessitating ever higher standards of precision and reliability. However, during prolonged operation, robotic manipulator joints experience friction due to factors such as wear, lubrication failure, and corrosion [2]. Joint friction exhibits strong nonlinear characteristics, and failure to accurately describe it can lead to inaccuracies in the robotic manipulators dynamic model. Employing an inaccurate dynamic model during control processes can decrease the reliability and precision of the robotic manipulators, posing challenges in manufacturing and potentially becoming a significant risk to production safety and product quality. Therefore, it is imperative to establish precise models of joint friction in robotic manipulators to accurately depict its nonlinear properties [3].

Common friction models for robotic manipulator joints include Coulomb friction model, Coulomb friction model with linear viscous, Stribeck friction model, Dahl friction model,

and LuGre friction model [4]. The Dahl and LuGre models are typical dynamic friction models, which exhibit good descriptive accuracy at low speeds. However, their complex structure, numerous parameters, and undetermined intermediate variables make it difficult to ensure the accuracy of friction torque acquisition, particularly in complex operating conditions, posing significant challenges for parameter identification [5]. Therefore, many scholars opt to describe joint friction in robotic manipulators based on static friction models. For instance, Shan et al. [6] employ the Coulomb friction model to describe the friction of the 3SPS+1PS parallel mechanism artificial hip joint. Zhang et al. [7] propose a "Coulomb + viscous" friction model for joint friction description. Although Coulomb and viscous Coulomb models can to some extent reflect the friction of robotic manipulator joints, they struggle to describe the nonlinear characteristics of friction and discontinuous friction torque at low speeds. References [8-9] introduce the arctangent function and sigmoid function into the viscous Coulomb friction model to address the discontinuous friction torque issue at low joint speeds, but they fail to consider the nonlinear characteristics of joint motion at low speeds. Bo et al. [10] consider the nonlinear characteristics of friction during low-speed joint motion and establish the Stribeck friction model. Stribeck is a typical static friction model that can effectively describe the joint friction of robotic manipulators. Its simple structure, wide applicability, and absence of difficult-to-measure intermediate state variables make it highly reliable. Hensen [11] compares and analyzes the experimental results of the static friction model Stribeck and the dynamic friction model LuGre, with the inclusion of zero-speed interval, finding that both models produce similar limit cycle oscillation effects in the system. Moreover, the Stribeck model can approximate the real friction force in the low-speed region with an accuracy of 90%, demonstrating high reliability. Considering these advantages, this paper selects the Stribeck model, which has low computational cost and high real-time performance, to describe the friction characteristics of robotic manipulator joints.

Although existing friction models can qualitatively describe the relationship between joint angular velocity and friction torque, the accurate identification of friction model parameters is crucial for establishing an accurate friction model. Inaccurate parameter identification can lead to issues such as jitter during robotic manipulators motion, affecting

This work was supported by the National Natural Science Foundation of China under Grant No. U2241263.

Di Luo is with the Jianghuai Advance Technology Center, Hefei, China (e-mail: 1274767387@qq.com).

Zhiqin Cai is with the Department of Engineering Mechanics, Dalian University of Technology, Dalian, China (e-mail: zhqcai@dlut.edu.cn).

Da Jiang is with the National Engineering Laboratory for Wheeled Vehicle, China North Vehicle Research Institute, Beijing, China (e-mail: ziangdar@sina.com)

Haijun Peng is with the Department of Engineering Mechanics and State Key Laboratory of Structural Analysis, Optimization and CAE Software for Industrial Equipment, Dalian University of Technology, Dalian, China (e-mail: hjpeng@dlut.edu.cn).

both the accuracy and stability of the manipulators [12]. Hence, numerous scholars have proposed various methods for friction model parameter identification. However, the accuracy of the original model is compromised during the approximation process. Vakil et al. [13] propose a nonlinear optimization problem derived from the principle of work energy to determine friction parameters, yet this method heavily relies on the model and lacks accuracy in parameter identification with noisy data. References [14-18] suggest using improved GA, cooperative coevolution grey wolf algorithms, PSO methods, and enhanced firefly algorithms for friction model parameter identification. However, these heuristic search algorithm approaches require setting initial values and range intervals based on prior experience, demanding high expertise and risking local optima, with weak resistance to interference. Many scholars [19-20] utilize neural network methods to fit friction forces, accurately establishing friction models, yet this approach requires a large amount of data and is susceptible to the quality of collected data.

With the advancement of machine learning and deep learning, Raissi from Brown University [21] proposed a PINN framework based on physical information, applying it to solve both forward and inverse problems of partial differential equations. The foundational idea of PINN is to integrate physical equations into the loss function of neural networks, thus obtaining neural networks constrained by physical models. Since its introduction, PINN has gained widespread recognition in fields such as fluid dynamics, thermodynamics, and material mechanics.

The paper presents a friction model parameter identification method based on PINN, integrating friction model information into the structure of the neural network loss function to constrain the parameter identification process with physical information. To validate the proposed approach, simulations were conducted and compared against GA and PSO. Furthermore, the effectiveness of the method was further demonstrated by contrasting it with purely data-driven friction modeling algorithms.

II. SYSTEM FOR MATHEMATICAL MODELING

A. Dynamics model of robotic manipulators

The following equation is employed to model the dynamics of two-degree-of-freedom robotic manipulators:

$$\mathbf{M}(\mathbf{q})\ddot{\mathbf{q}} + \mathbf{C}(\mathbf{q}, \dot{\mathbf{q}})\dot{\mathbf{q}} + \mathbf{G}(\mathbf{q}) = \boldsymbol{\tau} + \boldsymbol{\tau}_f + \boldsymbol{\tau}_d \quad (1)$$

where $\mathbf{q} \in R^{2 \times 1}$ is the joint angle vector of the manipulator, $\dot{\mathbf{q}} \in R^{2 \times 1}$ is the angular velocity vector of the manipulator, $\ddot{\mathbf{q}} \in R^{2 \times 1}$ is the angular acceleration vector of the manipulator, $\mathbf{M}(\mathbf{q}) \in R^{2 \times 2}$ is the mass inertia matrix, $\mathbf{C}(\mathbf{q}, \dot{\mathbf{q}})$ is the Coriolis force and the centrifugal force vector, $\mathbf{G}(\mathbf{q}) \in R^{2 \times 1}$ is the gravity vector, $\boldsymbol{\tau}_f \in R^{2 \times 1}$ is the vector of non-linear friction, $\boldsymbol{\tau}_d \in R^{2 \times 1}$ is the timing-varying external disturbance, and $\boldsymbol{\tau} \in R^{2 \times 1}$ is the torque vector acting on the joint.

B. Stribeck friction model of robotic manipulator joints

In this paper, Stribeck model with low computational cost and high real-time performance is selected to describe the frictional characteristics of the robot manipulator joint. The

mathematical expression of Stribeck friction model is as follows:

$$\boldsymbol{\tau}_f = \left(f_c + (f_s - f_c)e^{-\left(\frac{\dot{\mathbf{q}}}{v_s}\right)^2} \right) \text{sgn}(\dot{\mathbf{q}}) + f_v \dot{\mathbf{q}} \quad (2)$$

where $\boldsymbol{\tau}_f$ represents the frictional torque, $\dot{\mathbf{q}}$ is the angular velocity, f_c is the Coulomb friction force, f_s is the maximum static friction force, v_s is the threshold velocity for the Stribeck effect, f_v is the viscous friction coefficient. Considering the different friction model parameters for the robotic manipulators joint during forward and reverse motion, the equation is rewritten as follows:

$$\boldsymbol{\tau}_f = \begin{cases} \left(f_c^+ + (f_s^+ - f_c^+)e^{-\left(\frac{\dot{\mathbf{q}}}{v_s^+}\right)^2} \right) \text{sgn}(\dot{\mathbf{q}}) + f_v^+ \dot{\mathbf{q}}, \dot{\mathbf{q}} > 0 \\ \left(f_c^- + (f_s^- - f_c^-)e^{-\left(\frac{\dot{\mathbf{q}}}{v_s^-}\right)^2} \right) \text{sgn}(\dot{\mathbf{q}}) + f_v^- \dot{\mathbf{q}}, \dot{\mathbf{q}} < 0 \end{cases} \quad (3)$$

where $\dot{\mathbf{q}} > 0$ indicates counterclockwise motion of the robotic manipulator joint, $\dot{\mathbf{q}} < 0$ indicates clockwise motion of the robotic manipulator joint. Equation (3) enables the establishment of the Stribeck curve as a relationship between angular velocity and friction torque. Based on the Stribeck curve, it is possible to identify the eight parameters $f_c^+, f_s^+, v_s^+, f_v^+, f_c^-, f_s^-, v_s^-, f_v^-$ in the equation. In the Stribeck friction model, the parameters f_c^+, f_s^+, v_s^+ and f_v^+ represent the characteristics associated with the forward motion of robotic manipulators, while the parameters f_c^-, f_s^-, v_s^- and f_v^- denote the corresponding characteristics during the reverse motion.

III. PINN FRICTION MODEL PARAMETER IDENTIFICATION

The paper focuses on describing joint friction in robotic manipulators using the Stribeck model and proposes a parameter identification method based on PINN. Considering the inconsistency of parameters in the Stribeck friction model during forward and reverse motions, the paper presents a framework for solving the Stribeck model parameters using PINN, as illustrated in Fig. 1.

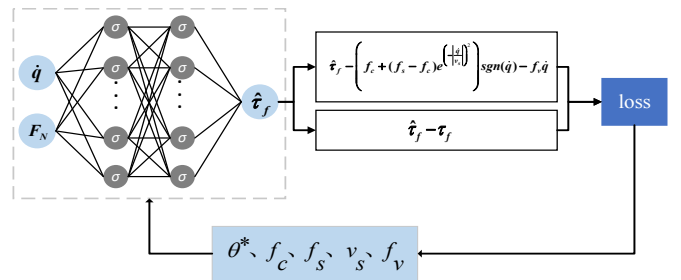


Fig. 1 PINN identification of Stribeck friction model parameters

Since joint friction in robotic manipulators primarily depends on the angular velocity $\dot{\mathbf{q}}$ and the normal pressure F_N , these variables are used as inputs. Through an artificial neural network, the predicted friction torque is outputted. The errors between the predicted friction torque $\hat{\boldsymbol{\tau}}_f$ and the actual friction torque $\boldsymbol{\tau}_f$ are defined as L_{data} .

$$L_{data} = \text{mse}(\hat{\boldsymbol{\tau}}_f - \boldsymbol{\tau}_f) \quad (4)$$

Additionally, the predicted friction torque $\hat{\tau}_f$ must satisfy the characteristics of the Stribeck friction model. The errors between the predicted friction torque $\hat{\tau}_f$ and the Stribeck friction model is denoted as L_{model} .

$$L_{model} = \text{mse}(\hat{\tau}_f - \left(f_c + (f_s - f_c)e^{-\frac{|\dot{q}|}{v_s}} \right) \text{sgn}(\dot{q}) - f_v \dot{q}) \quad (5)$$

Finally, the PINN total loss L_{total} is obtained by summing L_{data} and L_{model} .

$$L_{total} = L_{data} + L_{model} \quad (6)$$

The aforementioned loss functions are defined, and the parameters of the neural network and the eight parameters in the Stribeck model are updated using the gradient descent method.

IV. SIMULATION VALIDATION

A. Comparison and Validation of Parameter Identification Using Noise-Free Data

To compare the effects of parameter identification, this study considers the identification of eight parameters for the friction model of a single joint of the robotic manipulators, the parameters of the Stribeck model are set as shown in Table I.

TABLE I. Stribeck friction model parameter Settings

Parameter	Value	Parameter	Value
f_c^+	0.15	f_c^-	0.20
f_s^+	0.60	f_s^-	0.70
v_s^+	0.05	v_s^-	0.05
f_v^+	0.02	f_v^-	0.03

The velocity of the robotic manipulator joint is sampled at intervals of 0.05rad/s within the range of [-1rad/s, 1rad/s]. After simulation, 41 sets of noise-free data are obtained. The data acquisition process is shown in the Fig. 2.

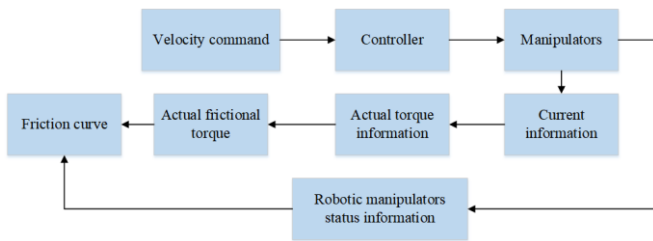


Fig.2 Friction data acquisition process

By obtaining the actual torque information from the current signals of the motor during the actual operation of the robotic manipulators, and then subtracting the theoretically calculated torque information, one can derive the frictional torque information.

TABLE II. Network parameter setting

Layer	Input nodes	Output nodes	Activation function
1	2	20	Tanh
2	20	20	Tanh
3	20	20	Tanh
4	20	1	Tanh

When using PINN for identification, the parameters of the network structure are shown in Table II. The training is set to 50,000 iterations with a learning rate of 0.001. Select the appropriate parameter after several parameter adjustments. The parameter variations during the identification process using PINN are depicted in Fig. 3.

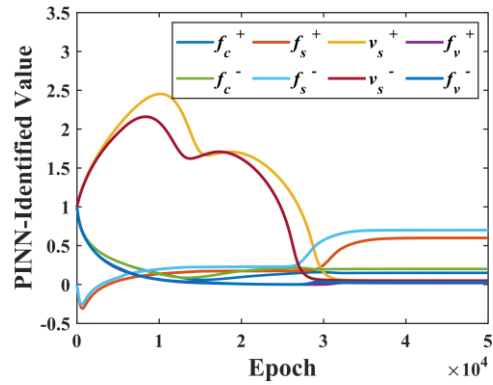


Fig. 3 Parameter change curve in the process of PINN

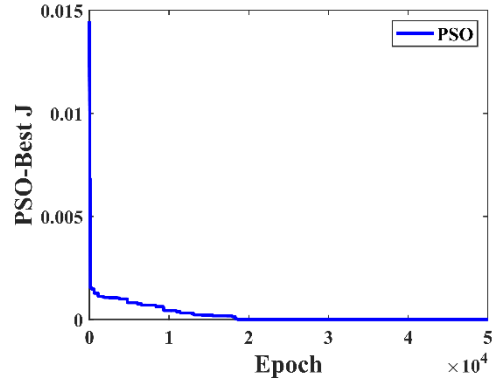


Fig. 4 Adaptive fitness variation in PSO

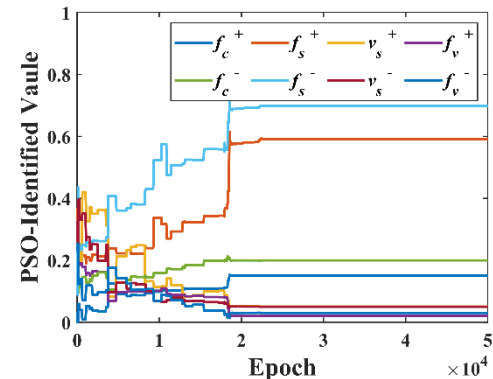


Fig. 5 Parameter change curve in the process of PSO

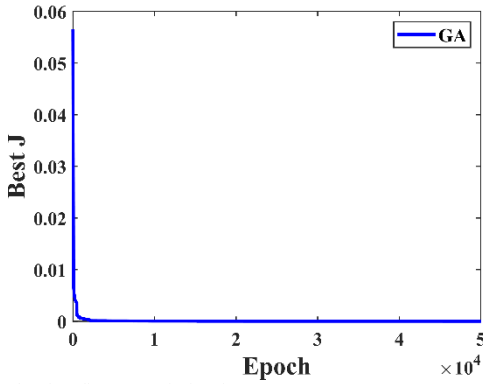


Fig. 6 Adaptive fitness variation in GA

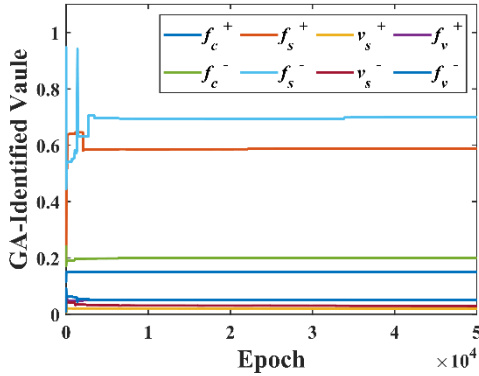


Fig. 7 Parameter change curve in the process of GA

To demonstrate the effectiveness of the proposed algorithm, comparisons are made with PSO and GA. When employing PSO for parameter identification, the parameters are set according to [16]. The population size is set to 100, the identification iterations are set to 50,000, and the learning factor is set to 1 with a minimum value of 0. The maximum values for the parameters are set to [1, 1, 0.1, 0.1, 1, 1, 0.1, 0.1].

For GA identification, the population size is set to 100, the number of iterations is set to 50,000, and the search boundaries are set the same as those for PSO. The parameter variation during the identification process is depicted in Figs. 4-7. The results of the three identification algorithms are summarized in Tables III-IV.

From the Figs. 4-7, it can be observed that the PSO converges to a stable state after 20,000 iterations, while the GA requires only 5,000 iterations to achieve convergence to a stable state.

From the comparison in the table above, it is evident that the maximum identification error rate for PINN is 1.40%, which is lower compared to both PSO and GA. The average error rates for the three methods are summarized in Table IV. The average error rate for PINN is 0.4375%, which represents a reduction of 31.2% and 38.2% compared to PSO and GA, respectively. This indicates that PINN-based identification exhibits higher accuracy, and moreover, it eliminates the need to determine the identification parameter range.

TABLE III. Comparison of the identification results of friction parameters in forward motion

Method	Real-Value				
	f_c^+	f_s^+	v_s^+	f_v^+	
PSO	Real-Value	0.15	0.60	0.05	0.02
	Value	0.14992	0.59125	0.05050	0.02013
	Error /%	0.0533	1.4570	1.0074	0.6448
GA	Real-Value	0.15	0.60	0.05	0.02
	Value	0.14976	0.58847	0.05068	0.02032
	Error /%	0.1543	1.9220	1.6134	1.3606
PINN	Value	0.15016	0.60124	0.04991	0.01972
	Error /%	0.1067	0.2068	0.1700	1.4000

TABLE IV. Comparison of the identification results of friction parameters in reverse motion

Method	Real-Value				
	f_c^-	f_s^-	v_s^-	f_v^-	
PSO	Real-Value	0.20	0.70	0.05	0.03
	Value	0.19977	0.69804	0.05011	0.03039
	Error /%	0.1144	0.22793	0.2261	1.3052
GA	Real-Value	0.20	0.70	0.05	0.03
	Value	0.19994	0.69868	0.05007	0.03008
	Error /%	0.0271	0.1878	0.2537	0.1410
PINN	Value	0.20010	0.70359	0.04981	0.02976
	Error /%	0.0500	0.5000	0.4000	0.6667

TABLE V. Comparison of noiseless data identification results

Method	Average error rate	Average reduction
PSO	0.6359%	31.2%
GA	0.7075%	38.2%
PINN	0.4375%	

B. Comparison and Validation of Parameter Identification Using Noise Data

During the data collection process for friction torque on a real robotic manipulator, it is inevitable to encounter noise due to external disturbances and imprecise sensors. Therefore, it is necessary to perform parameter identification using friction data contaminated with noise. The same set of eight friction parameters as in the previous section is utilized. The velocity signal of the robotic manipulators is sampled at intervals of 0.01 rad/s within the range of [-1rad/s, 1rad/s], resulting in a total of 201 data points. Gaussian noise, accounting for 5% of the data, is added to the collected dataset.

The same PINN, PSO and GA were used to identify the parameters. Fig. 8 shows the dynamic change process of parameters during PINN identification. When PSO and GA are

used for identification, the parameter changes in the identification process of noisy data are shown in Figs. 9-12.

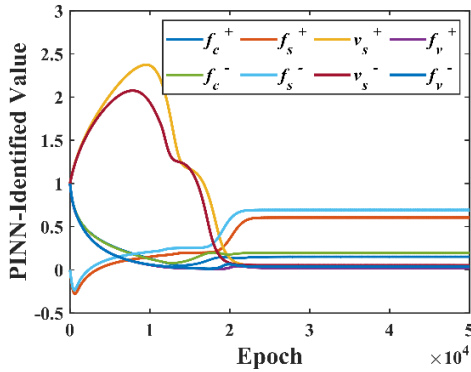


Fig. 8 Parameter change curve in the process of PINN

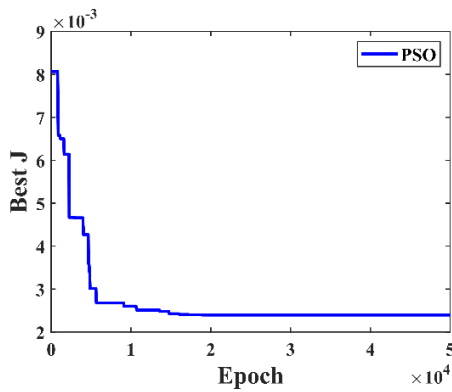


Fig. 9 Adaptive fitness variation in PSO

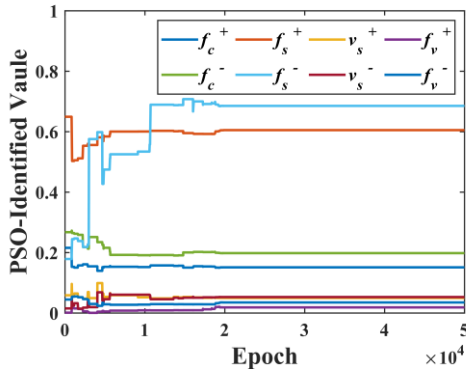


Fig. 10 Parameter change curve in the process of PSO

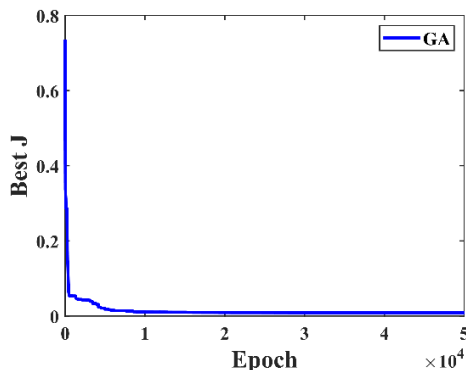


Fig. 11 Adaptive fitness variation in GA

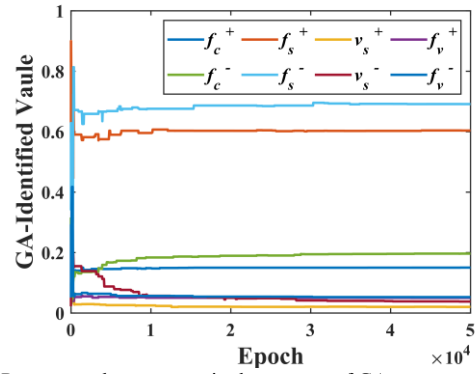


Fig. 12 Parameter change curve in the process of GA

Figs. 9-10 respectively depict the change in fitness values during the parameter identification process using PSO and GA. It can be observed that the PSO essentially reaches a plateau after 20,000 iterations, whereas the GA achieves stability after just 10,000 iterations.

TABLE VI. Comparison of the identification results of friction parameters in forward motion

Method	Real-Value				
	f_c^+	f_s^+	v_s^+	f_v^+	
PSO	Value	0.15097	0.60501	0.04976	0.01848
	Error /%	0.6461	0.8342	0.4720	7.6228
GA	Value	0.15106	0.60502	0.05028	0.02144
	Error /%	1.1672	0.8982	0.7302	13.5261
PINN	Value	0.15034	0.60377	0.05003	0.01954
	Error /%	0.2267	0.6283	0.0600	2.3000

TABLE VII. Comparison of the identification results of friction parameters in reverse motion

Method	Real-Value				
	f_c^-	f_s^-	v_s^-	f_v^-	
PSO	Value	0.19804	0.68521	0.05267	0.03479
	Error /%	0.9819	2.1132	5.3484	15.9732
GA	Value	0.19745	0.69114	0.05242	0.03553
	Error /%	1.1269	1.0455	4.4082	17.2978
PINN	Value	0.19830	0.69287	0.05181	0.03259
	Error /%	0.8500	1.0186	3.6200	8.6333

For more quantitative explanation, the comparison results of the three parameter identification methods are shown in Tables VI-VII.

From the Table VII, it can be observed that the maximum error rate for PINN identification is 8.6333%. Table VIII presents the average error rates for the three methods during identification with noisy data. The error rate of PINN is more than two times lower compared to both PSO and GA, indicating that PINN can achieve relatively accurate identification even with noisy data.

TABLE VIII. Comparison of identification results with noisy data

Method	Average error rate	Average reduction
PSO	4.2491%	49.1%
GA	5.0250%	56.9%
PINN	2.1671%	

V. CONCLUSION

This study focuses on identifying the parameters of the Stribeck friction model for robotic manipulator joints and proposes a parameter identification method based on PINN. In this method, the friction model with the parameters to be identified is introduced into the physical information part of PINN and incorporated as a regularization term in the loss function. The neural network's gradient descent optimization algorithm is employed to update the network parameters and the parameters to be identified in the friction model. Finally, the identified parameters are applied to the Stribeck model, resulting in a comprehensive Stribeck friction model for robotic manipulator joints.

The validation results demonstrate that in the identification of noise-free data, the PINN exhibits higher accuracy compared to GA and PSO, with an average identification error rate of 0.4375%. For data containing noise, the PINN achieves an average reduction of 50% in error rate compared to the GA and PSO. Additionally, this method does not require providing a range for the parameters to be identified. In the identification process of data with noise, the PINN also demonstrates higher precision compared to GA and PSO, indicating good robustness. Future work will mainly focus on parameter identification using experimental friction data and enhancing the performance of PINN parameter identification.

REFERENCES

- [1] S. Chung. "Post corona virus and 4th industrial revolution," *Journal of Material Science and Engineering Bo*, vol.10(4), pp.148-152, 2022.
- [2] S. Duan, H. Duan, X. Han, C. Li, H. Ouyang, Y. Li and G. Liu. "Inverse of key parameters of nonlinear friction model of robot joints," *Chinese Journal of Theoretical and Applied Mechanics*, vol.54(11), pp.3189-3202, 2022.(in Chinese)
- [3] S. YEH, H. SU. "Development of friction identification methods for feed drives of CNC machine tools," *The International Journal of Advanced Manufacturing Technology*, vol.52, pp.263-278, 2011.
- [4] F. Marques, P. Flores, P. Claro, J.C and et al. "A survey and comparison of several friction force models for dynamic analysis of multibody mechanical systems," *Nonlinear Dynamic*, vol.86, pp.1407-1443, 2016.
- [5] L. Liu, H. Liu and Z. Wu. "An Overview of Friction Models in Mechanical Systems," *Advance in Mechanics*, vol.2, pp.201-213, 2008.

- [6] X. Shan, G. Cheng. "Explicit Dynamic Modeling of a 3SPS+1PS Parallel Manipulator with Joint Friction," *Journal of Mechanical Engineering*, vol.53(01), pp.28-35, 2017.
- [7] Y. Zhang, P. Jin, J. Gong and Q. Liu. "Dynamic Modeling of 3-RPS Parallel Robot Considering Joint Friction," *Transactions of the Chinese Society of Agricultural Machinery*, vol.49(09), pp.374-381, 2018. (in Chinese)
- [8] M. Grotjahn, M. Daemi and B. Heimann. "Friction and rigid body identification of robot dynamics," *International Journal of Solids and Structures*, vol.38, pp.10-13, 2001.
- [9] Y. Tao, F. Zhao and J. Cao. "Research on Friction Characteristics Identification and Compensation of Cooperative Robot's Joints," *Modular Machine Tool & Automatic Manufacturing Technique*, vol.04, pp.28-31, 2019.
- [10] C. Li, D. Pavelescu. "The friction-speed relation and its influence on the critical velocity of stick-slip motion," *Wear*, vol.82(3), pp.277-289, 1982.
- [11] R.H.A. Hensen, M.J.G. van de Molengraft and M. Steinbuch. "Friction induced hunting limit cycles: a comparison between the LuGre and switch friction model," *Automatica*, vol.39(12), pp.2131-2137, 2003.
- [12] M. R. Kermani, M. Wong, R. V. Patel, M. Moallem and M. Ostojic. "Friction compensation in low and high-reversal-velocity manipulators," in *IEEE International Conference on Robotics and Automation (ICRA)*, New Orleans, LA, USA, vol.5, pp.4320-4325, 2004.
- [13] M. Vakil, R. Fotouhi and Nikiforuk P N. "Energy-based approach for friction identification of robotic joints," *Mechatronics*, vol.21(3): pp.614-624, 2011.
- [14] J. Bai, L. Fan, S. Zhang and et al. "The parameter identification model considering both geometric parameters and joint stiffness," *Industrial Robot: the international journal of robotics research and application*, vol.47(1), pp.76-81, 2019.
- [15] T. Zhang, L. L. Hu and Y. B. Zou. "Identification of improved friction model for robot based on hybrid genetic algorithm," *Journal of Zhejiang University (Engineering Science)*, vol.55(05), pp.801-809+854, 2021. (in Chinese)
- [16] G. L. Li, H. L. Li and Q. J. Wang. "Stribeck friction model parameter identification for a permanent-magnet spherical motor," *Electric Machines and Control*, vol.26(04), pp.121-130, 2022. (in Chinese)
- [17] J. K. Cui, H. Y. Sai and E. Y. Zhang. "Identification and compensation of friction for modular joints based on grey wolf optimizer," *Optics and Precision Engineering*, vol.29(11), pp.2683-2691, 2021.
- [18] B. W. Gao, W. Shen and Y. Dai. "Parameter identification and compensation of a friction model based on improved glowworm swarm optimization," *Journal of Vibration and Shock*, vol.42(06), pp.69-78, 2023.
- [19] X. Tu, Y. Zhou, P. Zhao and et al. "Modeling the Static Friction in a Robot Joint by Genetically Optimized BP Neural Network," *Journal of Intelligent and Robotic Systems*, vol.94, pp.29-41, 2019.
- [20] H. Peng, N. Song, F. Li, and S. Tang. "A Mechanistic-Based Data-Driven Approach for General Friction Modeling in Complex Mechanical System," *Journal of Applied Mechanics-Transactions of the Asme*, vol.89(7), pp.071005, 2022.
- [21] M. Raissi, P. Perdikaris and G.E. Karniadakis. "Physics-informed neural networks: A deep learning framework for solving forward and inverse problems involving nonlinear partial differential equations," *Journal of Computational Physics*, vol.378, pp.686-707, 2019.